Dynamic Simulation of an Innovative Compressed Air Energy Storage Plant - Detailed Modelling of the Storage Cavern

LASSE NIELSEN
Technische Universität Braunschweig and
Energy Research Centre Lower Saxony in Goslar
Institute for Heat- and Fuel Technology
Franz-Liszt-Straße 35, D-38106 Braunschweig
GERMANY
lasse.nielsen@tu-bs.de

REINHARD LEITHNER
Technische Universität Braunschweig
Institute for Heat- and Fuel Technology
Franz-Liszt-Straße 35, D-38106 Braunschweig
GERMANY
r.leithner@tu-bs.de

Abstract: An innovative concept of an compressed air energy storage (CAES) plant is developed at the Institute for Heat- and Fuel Technology (IWBT) of the Technische Universität Braunschweig. This concept aims to minimise the negative aspects of state-of-the-art CAES-plants and is named isobaric adiabatic compressed air energy storage plant with combined cycle (ISACOAST-CC). To increase the storage efficiency, one aspect of this concept is to reduce compressor losses due to high differences of the storage pressure within the cavern by the use of a brine shuttle pond at the surface to drive out the stored air at nearly constant pressure.
The main focuses in the presented article are the modelling and the calculation results of the simulation of the isobaric air storage cavern which is used in this concept. Furthermore, the results of a complete dynamic simulation of an ISACOAST-CC cycle are presented. The storage efficiency as well as plant efficiency and specific storage capacity are calculated.

Key–Words: Compressed Air Energy Storage (CAES), Enbipro, Dynamic simulation, Underground salt cavern

1 Introduction

Due to the worldwide rising energy consumption, the negative aspects of the present structure of power supply are becoming more significant. The finite nature and unequal distribution of fossile fuels and the decrease of CO_2-production is challenging the energy industry concerning supply guarantee and price stability in future. Besides the improvement of efficiency, the application of renewable energy is helping to solve these issues. Wind energy has the highest potential as a significant assistance to ensure future power supply [1]. Due to the the rising amount of produced wind energy in Germany, future adjustments of the grid infrastructure become necessary. The characteristic of wind energy is, that the converted power is fed in fluctuating and is not always available when it is needed. At present the required regulating power is provided mainly by fossile-fired power plants in partload mode resulting in lower efficiency and higher material wear as a result of fluctuating operating temperatures. Energy storage facilities can be used to provide positive and negative regulating power, reduce the amount of inefficient part load fossile-fired power plants and raise the efficiency, stability and durability of the whole power generation network.

1.1 Compressed Air Energy Storage Plants

One type of energy storage plant which is able to buffer large amounts of renewable electric energy is the so called CAES-plant. Worldwide there are two CAES-plants in operation, one in McIntosh, Alabama (USA) and one in Huntorf, Germany. However, there are still several concepts in design state. In general

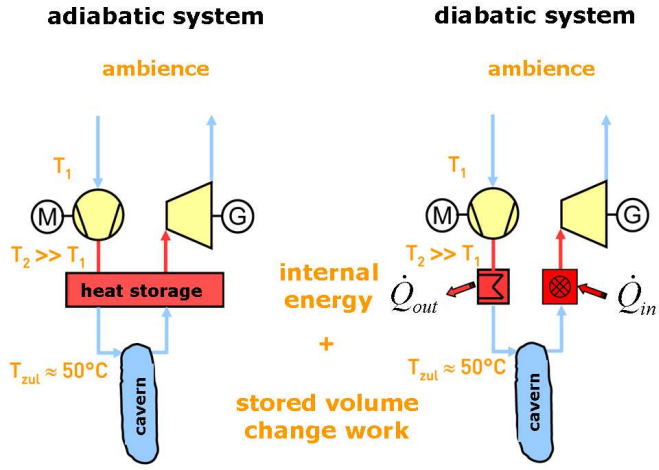

Figure 1: Adiabatic and diabatic CAES concepts [3]

there are two different concepts, the adiabatic and di-

abatic CAES as shown in figure 1. By taking energy out of the grid, a compressor is driven by an electric motor to store air in underground salt caverns. When energy is needed at peak load time the air is expanded in a gas or air turbine. The difference between these concepts is the heat storage and the combustion chamber. Due to inlet temperature limitations for stability reasons of the cavern the air needs to be cooled down before it enters the cavern. At the Huntorf-plant the air is cooled down by heat exchange to the environment without using a heat storage. In discharge mode the air is heated up by burning natural gas in a combustion chamber to reach the needed turbine inlet temperature. At the McIntosh-plant in discharge mode, the air is pre-heated additionally with the exhaust gas in a recuperator, thus reducing the consumption of natural gas. However the efficiency of state-of-the-art CAES-plants with 41,8 % (Huntorf) and 53,8 % (McIntosh) [2] is very low in comparison with pumped hydro plants i.a. due to the air cooling losses. The adiabatic concept stores the heat from the hot compressed air in a heat storage before the air enters the cavern. In discharge mode the air flows through the heat storage again and is heated up to the turbine inlet temperature without fuel consumption. There is no adiabatic CAES built at present but it shall reach storage efficiencies of around 70 % [3]. A negative aspect of this concept is, that every heat storage has ambient losses and a temperature breakthrough curve. The turbine inlet temperature can not be ensured over the whole discharging time. Due to the decreasing turbine inlet temperature, the pressure difference which is expanded in the turbine needs to be downsized to avoid that the turbine outlet temperature gets too low. Therefore the power output is reduced with progressing discharging time. Both concepts use a salt cavern with constant volume. A negative aspect of such a cavern is, that the air is stored at a higher pressure than the inlet pressure of the turbine to reach long discharging times. At Huntorf, for example, the air is stored with up to 72 bar while the high pressure-turbine needs an inlet pressure of 41 bar. Hence the air has to be throttled before entering the turbine which results in a decreased efficiency.

1.2 Concept developed at the IWBT

In general the concept developed at the Institute for Heat- and Fuel Technology is a combination of the adiabatic and the diabatic process, because it uses a heat storage and a combustion chamber. The schematic diagram in figure 2 shows the design of the ISACOAST-CC concept. This new CAES system differs from existing ones, by the use of a brine shuttle pond at the surface which enables to operate the

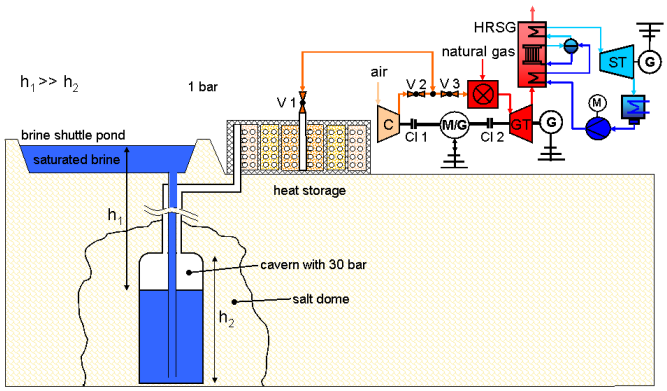

Figure 2: Schematic diagram of the ISACOAST-CC-concept [4]

air storage nearly isobarically. In storage mode the compressor of a state-of-the-art gas turbine is driven by a motor/generator, the turbine is decoupled and the brine is driven out of the cavern into the shuttle pond by the compressed air. This process takes place at nearly constant pressure. While state-of-the-art CAES suffer from efficiency losses due to pressure variation, losses of this type are avoided in this concept since it is operated at nearly constant pressure. Before entering the cavern, the heat of the air, resulting from the compression, is stored in a special heat storage. This unit consists of a large number of pressure resistant helical steel tubes that transfer the heat to the surrounding material (at atmospheric pressure). In discharge mode, the compressed air flows from the cavern to the combustion chamber of a state-of-the-art gas turbine. By passing through the heat storage, the air is heated up nearly to the compressor outlet temperature again. As a result, there is nearly no difference between air from the storage and air from the compressor. The motor/generator is operated as a generator in discharge mode to convert the additional power which is consumed by the compressor –now decoupled– in regular operation of the gas turbine. This avoids duplication of equipment and redesign of the gas turbine shaft. A heat recovery steam generator (HRSG) is used to produce steam using the energy of the hot turbine exhaust gas for a steam cycle.

1.2.1 Advantages of the IWBT-Concept

The innovative approaches result in serveral advantages of this concept. It provides a high storage efficiency due to intermediate storage of compressor waste heat, a high system efficiency and constant power output during the whole discharging process due to the constant high turbine inlet temperature. Losses caused by the difference in turbine inlet pres-

sure and the high storage pressure from state-of-the-art CAES-plants are minimised by the nearly isobaric cavern and a storage pressure slightly above turbine inlet pressure. The minor pressure and temperature fluctuation allow a high stability and durability of the cavern. Standard gas turbines with combined cycle and high efficiencies are used. The stored electrical energy is nearly doubled due to the co-firing with natural gas. This is an important factor during extreme wind calms. Furthermore, the whole plant is able to operate flexibly without storages as a standard gas turbine with combined cycle for generation of peak-load electricity. The storage capacity and discharging time is increased remarkably compared to state-of-the-art CAES-plants, i.a. by the reason that the total air inside the cavern can be used to generate electricity unlike caverns with constant volume.

The discharge time depending on depth of the bottom and the volume of the isobaric cavern are shown in diagram 3. The results are calculated with an air inlet mass flow of 634 $\frac{kg}{s}$ of an Alstom GT-26. In

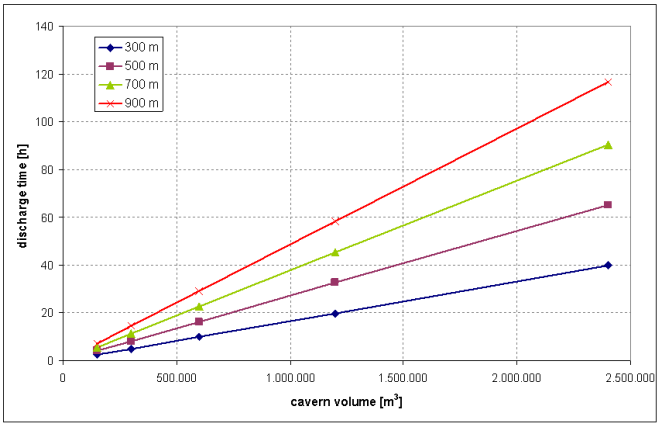

Figure 3: Discharge time of an isobaric cavern with brine shuttle pond in operation with an Alstom GT-26

comparison to this, the discharge operation from the CAES-plant Huntorf lasts two hours. If it would be operated with a brine shuttle pond, the discharging time could be increased up to 19 hours.

2 Mathematical model of the isobaric cavern

The plant is simulated with the software ENBIPRO (ENergie BIlanz PROgramm / energy balance program) which is used for stationary and dynamic simulation of power plant cycles and has been developed at the IWBT [5], [6], [7], [8]. The different component models constist of balance and transport equations (mass, energy, etc.) and substance property calculations. This article presents the modelling and the simulation results of the isobaric cavern used in the ISACOAST-CC concept.

The model describes an underground excavation in a salt dome created by solution mining. The cavern is linked to the surface by two boreholes with inner pipings or one borehole with two concentric pipes from which one is the connection between the brine shuttle pond to the air storage and reaches down to the bottom of the cavern. The other one, ending at the top of the cavern, is used for the transport of the compressed air which is driven out of the cavern to the surface by the brine. The brine column between cavern and shuttle pond creates a nearly isobaric pressure level which varies only by the difference in the geodetic height resulting out of the changing brine filling level inside the cavern. The pressure of the air inside the storage equals the resulting pressure of the brine. Additional equations are implemented to calculate the pressure losses out of initially given pressure loss coefficients. Two volumes (brine, air) are linked by an isochoric equation and the in- and outlets affect these in form of the ideal gas law and a simple volume calculation for the incompressive brine. The implemented energybalance of the air, according to the first law of thermodynamics, regards the change of the storage temperature resulting out of the changing pressure during the storage processes. The heat transfer between the two mediums and the cavern wall is described by nonstationary heat conduction in a semi-infinite body. With an input/output routine it is possible to set a given temperature field as initial value and write out the resulting temperature characteristics inside the wall. The model has separate in- and outlets for each medium to avoid that following components in a cycle simulation calculate with negative mass flows, since the direction of flow changes between charge and discharge operation. In reality the medium will flow in both directions through the boreholes or concentric pipes respectively.

2.1 Equationsystem

Constants:

$$g = 9,81\ \frac{m}{s^2} \quad (1)$$

$$R_a = 286,7\ \frac{J}{kgK} \quad (2)$$

$$c_{p,b} = 4169\ \frac{J}{kgK} \quad (3)$$

$$\varrho_b = 1174\ \frac{kg}{m^3} \quad (4)$$

$$p_{env} = 1,013\ bar \quad (5)$$

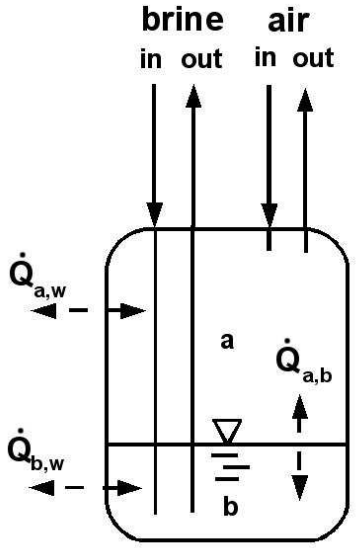

Figure 4: Schematic diagram of the cavern model

General:

$$T_m = \frac{(T+T_{ref})}{2}, \quad T_{ref} = 298,15\ K \tag{6}$$

$$c_{p,m} = f(T_m, p) \tag{7}$$

Mass balances:

$$\frac{dm_a}{dt} = -\dot{m}_{a,out} + \dot{m}_{a,in} \tag{8}$$

$$\frac{dm_b}{dt} = -\dot{m}_{b,out} + \dot{m}_{b,in} \tag{9}$$

Volume calculation:

$$V_b = \frac{m_b}{\varrho_b} \tag{10}$$

$$V_a = \frac{m_a \cdot R_a \cdot T_a}{p_a} \tag{11}$$

Volume correlation with $V_c = const.$:

$$V_c = V_a + V_b \tag{12}$$

Energy balance:

The nonstationary energy balance is implemented according to the first law of thermodynamics for open systems as stated in [9]. The storage process is a polytropic change of condition because temperature, pressure and volume of the air are varying in every timestep. The index a for air is omitted for the purpose of clarity.

The general equation of the first law of thermodynamics for open systems:

$$\frac{d}{dt}\int_{V_{cv}} \varrho(u + \frac{v^2}{2} + gz)dV = \sum_k [\dot{m}(h + \frac{v^2}{2} + gz)]_k + \dot{Q} + \dot{W}_t - p\frac{dV_{cv}}{dt} \tag{13}$$

The technical work in this system is zero and the kinetic and potential energies are neglected. With the flow of volume-change work $\dot{W}_v = p\frac{dV_{cv}}{dt}$ the equation is reduced to:

$$\frac{d}{dt}\int_{V_{cv}} \varrho u dV = \sum_k [\dot{m}h]_k + \dot{Q} + \dot{W}_v \tag{14}$$

The density of the air inside the storage is regarded as constant along the cavern height and only one airmassflow is entering or leaving the volume, depending on the current storage process:

$$\frac{d(mu)}{dt} = \dot{m}h + \dot{Q} + \dot{W}_v \tag{15}$$

$$m\frac{du}{dt} + u\frac{dm}{dt} = \dot{m}h + \dot{Q} + \dot{W}_v \tag{16}$$

$$\frac{du}{dt} = \frac{\dot{m}h + \dot{Q} + \dot{W}_v - u\frac{dm}{dt}}{m} \tag{17}$$

The internal energy is calculated through the heat capacity at constant volume multiplied by the temperature difference of the actual and the reference temperature.

$$u = c_{v,m} \cdot \Delta T \tag{18}$$

$$u = (c_{p,m} - R_a) \cdot \Delta T \tag{19}$$

With

$$\Delta T = T - T_{ref} \tag{20}$$

follows:

$$(c_{p,m} - R_a)\frac{d\Delta T}{dt} = \frac{\dot{m}h + \dot{Q} + \dot{W}_v - (c_{p,m} - R_a) \cdot \Delta T\frac{dm}{dt}}{m} - \frac{d(c_{p,m} - R_a)}{dt}\Delta T \tag{21}$$

For small timesteps and with index i as the current timestep:

$$(c_{p,m,i} - R_a)\frac{\Delta\Delta T}{\Delta t} = \frac{\dot{m}h + \dot{Q} + \dot{W}_v - (c_{p,m} - R_a) \cdot \Delta T\frac{\Delta m}{\Delta t}}{m} - \frac{\Delta(c_{p,m} - R_a)}{\Delta t}\Delta T \tag{22}$$

with:

$$\Delta\Delta T = (T_i + T_{ref}) - (T_{i-1} + T_{ref}) \tag{23}$$

$$\Delta\Delta T = (T_i - T_{i-1}) \tag{24}$$

The formula is rearranged to give T_i:

$$T_i = \frac{\frac{\Delta m h_m + \Delta Q + \Delta W_v - (c_{p,m,i} - R_a)\cdot \Delta T \Delta m}{m_i}}{(c_{p,m,i} - R_a)} - \frac{\Delta (c_{p,m} - R_a)\Delta T}{(c_{p,m,i} - R_a)} + T_{i-1} \quad (25)$$

$$T_i = \frac{\frac{\Delta m h_m + \Delta Q + \Delta W_v - (c_{p,m,i} - R_a)\cdot \Delta T \Delta m}{m_i}}{(c_{p,m,i} - R_a)} - \frac{(c_{p,m,i} - c_{p,m,i-1})(T_i - T_{ref})}{(c_{p,m,i} - R_a)} + T_{i-1} \quad (26)$$

The volume-change work of a polytropic change of condition is defined as:

$$\Delta W_{v,pol} = \frac{p_i V_i - p_{i-1} V_{i-1}}{n_{pol} - 1} \quad (27)$$

with the polytropic exponent:

$$n_{pol} = \frac{ln \frac{p_i}{p_{i-1}}}{ln \frac{V_{i-1}}{V_i}} \quad (28)$$

The heat exchanged with brine and cavern wall between two timesteps is averaged:

$$\Delta Q = (\frac{\dot{Q}_{a,w,i} + \dot{Q}_{a,w,i-1}}{2} + \frac{\dot{Q}_{a,b,i} + \dot{Q}_{a,b,i-1}}{2}) \cdot \Delta t \quad (29)$$

like the exchanged enthalpy with the air mass flow (T_m averaged between two timesteps)

$$\Delta m h_m = \Delta m (c_{p,m}(T_m - T_{ref})) \quad (30)$$

The nonstationary energy balance of the air is calculated as followed:

$$T_i = \frac{\frac{\Delta m (c_{p,m}(T_m - T_{ref}) - (c_{p,m,i} - R_a)(T_i - T_{ref}))}{m_i}}{(c_{p,m,i} - R_a)} + \frac{\frac{\Delta Q + \frac{p_i V_i - p_{i-1} V_{i-1}}{n_{pol}-1}}{m_i}}{(c_{p,m,i} - R_a)} - \frac{(c_{p,m,i} - c_{p,m,i-1})(T_i - T_{ref})}{(c_{p,m,i} - R_a)} + T_{i-1} \quad (31)$$

Energy balance of the brine:

$$T_{b,i} = \frac{\Delta Q_{b,w} + \Delta Q_{a,b}}{m_{b,i} \cdot c_{p,b}} + \frac{\Delta m_b \cdot c_{p,b} \cdot (T_{b,in|out} - T_{ref})}{m_{b,i} \cdot c_{p,b}} + \frac{m_{b,i-1} \cdot c_{p,b} \cdot (T_{b,i-1} - T_{ref})}{m_{b,i} \cdot c_{p,b}} + T_{ref} \quad (32)$$

Temperature of the cavern wall:

The calculation of the cavern wall temperature is modelled with nonstationary heat conduction in a semi-infinite body according to [10]. It can be calculated with an initial balance or with a given distribution of temperatures. In the first case, the temperature-vector at timestep zero is overwritten with T_∞ and based on this the characteristics are calculated during the simulation. The basic equation used, is the differential equation of Fourier for constant heat conduction coefficients:

$$\frac{\partial T}{\partial \tau} = a \; div \; grad \; T + \frac{\tilde{\dot{q}}_i}{\varrho c_p} \quad (33)$$

Because no inner heat sources are located in the wall, the equation is reduced to:

$$\frac{\partial T}{\partial \tau} = a \; div \; grad \; T \quad (34)$$

and for the one dimensional case of an infinite cylinder:

$$\frac{\partial T}{\partial \tau} = a(\frac{\partial^2 T}{\partial r^2} + \frac{1}{r}\frac{\partial T}{\partial r}) \quad (35)$$

Figure 5 shows the scematic discretisation of the cavern wall. The temperature of the wall is located between two supporting points, whereby the approximation becomes more exact [10].

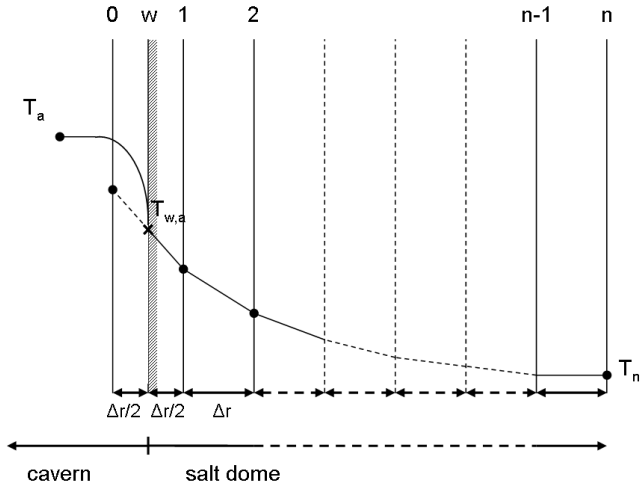

Figure 5: Discretisation of the cavern wall

For the implicit solution by using the rear differential quotient results the following equationsystem with the location coordinate j and the current timestep i. The numeric solution of this method allows the calculation of temperature compensation processes with any initial temperature characteristics and boundary

conditions of the 1st, 2nd and 3rd type which also can be time dependent [10].

$$\begin{aligned} -T_{j,i-1} &= Fo^{+}(1-r^{*})T_{j-1,i} \\ &-(1+2Fo^{+})T_{j,i}+Fo^{+}(1+r^{*})T_{j+1,i} \end{aligned} \quad (36)$$

$$\begin{aligned} T_{j,i} &= \frac{T_{j,i-1}}{(1+2Fo^{+})} \\ &+\frac{Fo^{+}((1-r^{*})T_{j-1,i}+(1+r^{*})T_{j+1,i})}{(1+2Fo^{+})} \end{aligned} \quad (37)$$

The dimensionless location coordinate r^* for cylindrical coordinates and the current location:

$$r^{*} = \frac{\Delta r}{2r_j} \quad (38)$$

The Fourier-number Fo^+ is equivalent to the relation of time according to thermical time constant exclusively at heat conduction in the wall [10]. For cylindrical coordinates with a as the conductibility of temperature for rock salt it is:

$$Fo^{+} = \frac{a_{rs}\Delta\tau}{\Delta r^{2}} \quad (39)$$

As basis for the calculation the 3rd boundary condition is chosen, because the temperature of the fluid is known and heat is transferred between medium and wall. As boundary condition for the other side at infinity of the salt dome T_n is set to T_∞. For the transition between fluid and wall the following boundary condition is applied:

$$T_{a,i}Bi^{+} = T_{0,i}(\frac{Bi^{+}}{2}+1)+T_{1,i}(\frac{Bi^{+}}{2}-1) \quad (40)$$

The lokal Biot-number Bi^+ physically describes the relation of heat conduction inside the wall to the heat transfer coefficient at the surface. It is calculated with the given heat transfer coefficient and the heat conductivity of rock salt.

$$Bi^{+} = \frac{\alpha_{a,w}\Delta r}{\lambda_{rs}} \quad (41)$$

The temperature of the wall between the supporting points 0 and 1 is calculated with the arithmetic mean of these two temperatures.

$$T_{w,a} = \frac{T_{0,i}+T_{1,i}}{2} \quad (42)$$

The distance Δr and the number of supporting points can be given in the properties of the component at the graphical user interface of ENBIPRO. The calculation of the brine sided wall is carried out in the same way with own temperature characteristics.

$$T_{w,b} = \frac{T_{0,i}+T_{1,i}}{2} \quad (43)$$

The heat transfer caused by the changing contact to air and brine respectively during the changing filling level of the cavern is neglected.

The equations for heat transport are calculated with constant heat transfer coefficients and the appropriate surfaces and temperatures:

$$\dot{Q}_{a,w} = \alpha_{a,w}\cdot A_{a,w}(T_{w,a}-T_a) \quad (44)$$

$$\dot{Q}_{a,b} = \alpha_{a,b}\cdot A_{a,b}(T_a-T_b) \quad (45)$$

$$\dot{Q}_{b,w} = \alpha_{b,w}\cdot A_{b,w}(T_{w,b}-T_b) \quad (46)$$

Calculation of the cavern cross section area:

$$A_{\emptyset} = \frac{\Pi}{4}\cdot d_c^{2} \quad (47)$$

Calculation of the cavern volume:

$$V_c = A_{\emptyset}\cdot H_c \quad (48)$$

The surfaces are calculated with an enlargement factor A_e which regards the fissures of the cavern walls.

$$A_{a,w} = (\pi\cdot d_c(H_c-z)+A_{\emptyset})A_e \quad (49)$$

$$A_{b,w} = (\pi\cdot d_c\cdot z+A_{\emptyset})A_e \quad (50)$$

The filling level of the cavern:

$$z = \frac{V_b}{A_{\emptyset}} \quad (51)$$

The pressures are calculated according to Bernoulli's equation. In this model the in- and outlet pressure of the brine is the pressure of the compressed air inside the cavern.

$$\begin{aligned} p_{a,c} &= p_{env}+\varrho_b\cdot g\cdot(H_d+H_c-z) \\ &-\zeta_b\cdot\frac{\varrho_b}{2}\cdot v_{b,in}^{2} \text{ for } \dot{m}_{a,out}>0 \end{aligned} \quad (52)$$

$$\begin{aligned} p_{a,c} &= p_{env}+\varrho_b\cdot g\cdot(H_d+H_c-z) \\ &+\zeta_b\cdot\frac{\varrho_b}{2}\cdot v_{b,out}^{2} \text{ for } \dot{m}_{a,in}>0 \end{aligned} \quad (53)$$

$$\begin{aligned} p_{a,out} &= p_{a,c}-\varrho_{a,m}\cdot g\cdot(H_d+H_c-z) \\ &-\frac{\varrho_{a,out,m}}{2}\cdot v_{a,out,m}^{2}\cdot(1+\zeta_a) \text{ for } \dot{m}_{a,out}>0 \end{aligned} \quad (54)$$

$$\begin{aligned} p_{a,in} &= p_{a,c}-\varrho_{a,m}\cdot g\cdot(H_d+H_c-z) \\ &-\frac{\varrho_{a,in,m}}{2}\cdot v_{a,in,m}^{2}\cdot(1-\zeta_a) \text{ for } \dot{m}_{a,in}>0 \end{aligned} \quad (55)$$

The links of temperature between storage and in- / outlet:

$$T_{a,out} = T_a \quad \text{for} \quad \dot{m}_{a,out}>0 \quad (56)$$

$$T_{b,out} = T_b \quad \text{for} \quad \dot{m}_{b,in}>0 \quad (57)$$

2.2 Simplifications and assumptions

The cavern model uses the following simplifications and assumptions:

- the air is considered as an ideal gas
- regarding of fissures of the cavern walls by an enlargement factor
- constant substance properties of the brine
- simulation with dry air
- no influence of pressure to substance properties
- no heat transfer between medium and tubings

3 Simulation

3.1 Dynamic simulation of a single cavern

A complete storage cycle (charge and discharge processes are simulated separately) starting with balanced temperatures (298,15 K) was taken as basis for the second cycle. The whole cavern is dimensionated as one of two caverns used in the ISACOAST-CC process as described in [11]. Regarding the pressure losses of the tubings, two boreholes are assumed per cavern and each medium. Table 1 and 2 show the initial and boundary values that are used for the second simulation of the discharge process.

Initial values of the second discharge process	
cavernvolume	133.847,66 m^3
volume of air	127.212,76 m^3
volume of brine	6.634,90 m^3
mass of air	6.785.946,5 kg
mass of brine	7.789.371,90 kg
filling level	2,85 m
temperature of air	311,32 K
temperature of brine	288,85 K
temperature of air-sided wall	309,71 K
temperature of brine-sided wall	288,96 K

Table 1: Initial values of the cavern

Figure 6 shows the massflows of air and brine over the entire simulation time of six hours. The curve progression of the air is raised slowly to the constant design value of 317 $\frac{kg}{s}$ and is equal for charging and discharging process. The massflow of the brine at the charging process results from the changing volume inside the cavern which is displaced by the influent air. At discharge process the air flow is held at the constant design value too and the influent brine shows a characteristic which results from the changing density of the air.

Boundary values of the second discharge process	
depth of cavern head	350 m
height of cavern	57,46 m
diameter of cavern	54,46 m
heat transfer coefficient air-wall	100 $\frac{W}{m^2K}$
heat transfer coefficient air-brine	1,531 $\frac{W}{m^2K}$
heat transfer coefficient brine-wall	743,12 $\frac{W}{m^2K}$
diameter of air tubing	0,7 m
diameter of brine tubing	0,7 m
pressure loss coefficient air tubing	10,87
pressure loss coefficient brine tubing	11,57

Table 2: Boundary values of the cavern

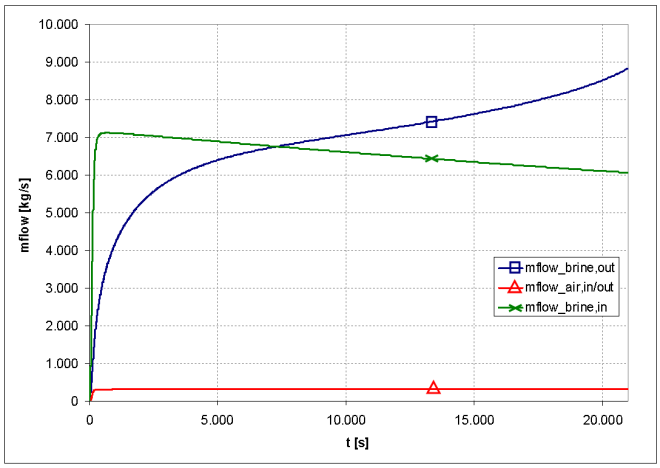

Figure 6: Massflows at charge and discharge process

As shown in figure 7, the pressure of the air inside the cavern and at the outlet (surface) are following the raising filling level and the pressure losses due to the raising massflows of air and brine.

Figure 8 shows the characteristics of the air temperature and density inside the cavern while discharging. Both values are influenced by the changing cavern pressures depending on the filling level and increasing pressure losses of the tubings when the massflows are rising as well as the heat losses from the air to the brine and the cavern walls. At beginning of the discharge process the temperature of the air is slightly higher than the temperature of the walls, but the effect of the heat transfer is marginal compared to the change of pressure. During the discharge process the temperature of the air is dropping beneath the wall temperature and at the end it is slightly heated up by the higher temperatures of the wall.

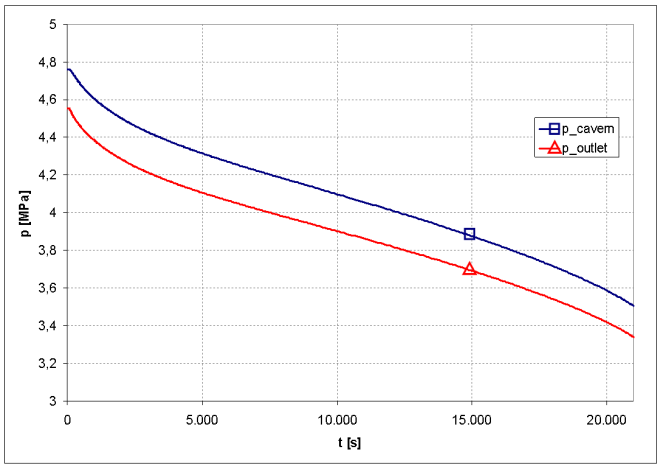

Figure 7: Pressures of air inside cavern and outlet

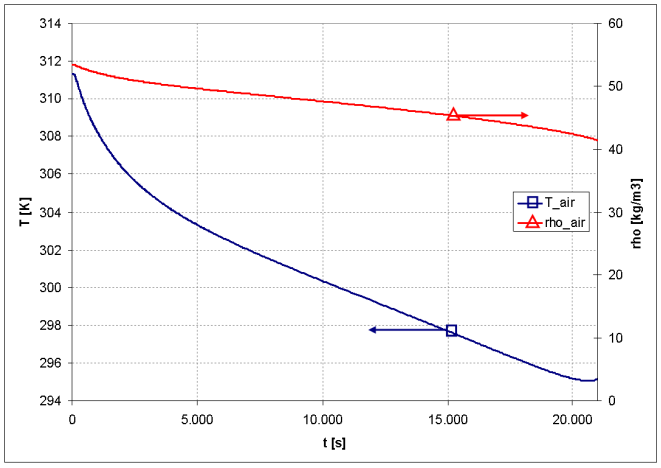

Figure 8: Temperature and density of the air at discharge process

The temperature characteristics inside the cavern wall next to the air at the end of the charge and the discharge process is shown in figure 9. The influenced length is set to one metre inside the salt dome and is divided into 100 supporting points. The value at location 0 represents the wall and the one at -1.5 cm the air temperature.

3.2 Dynamic simulation of an ISACOAST-CC storage cycle

A complete storage cycle of an ISACOAST-CC concept was simulated with a less detailed version of the cavern without nonstationary heat conduction inside the cavern walls. The temperature of the surrounding walls was regarded as constant resulting in higher heat losses of the stored air. The plant was designed for a storage period of six hours using an Alstom GT-26 in

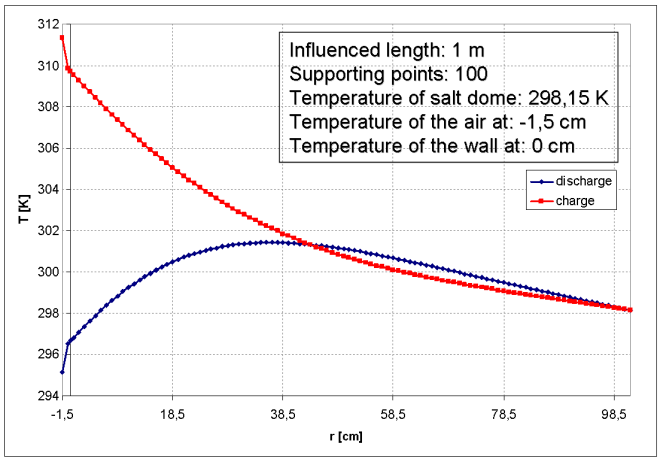

Figure 9: Temperatures of the cavern-wall at the end of the charge and discharge process

combined cycle mode and two caverns with a volume of 132.000 m^3 each. An additional compressor is used to overcome the pressure losses of the tubings and the change of the geodetic height of the brine column during the process. The heat storage was divided into ten layers insulated from each other to realise a layering of the storage temperature. Due to the decreasing outlet temperature of the heat storage during discharge, an additional combustion chamber is used to raise the air temperature up to the designed inlet value of the first GT-26 combusting chamber. The aim was to create the same thermal properties ahead the GT-26 combustion chamber as they are in operation without any storages like a conventional gas turbine combined cycle. In reality this additional compressor and combustion chamber will be combined with the original ones. The whole simulated configuration with results is shown in figure 10.

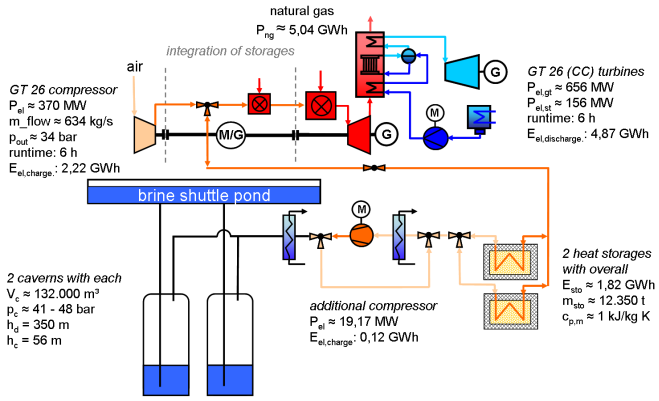

Figure 10: Schematic diagram and results of a 6 h storage concept [4]

The performance of a storage plant is described by the storage efficiency and is calculated by the ratio of the energy gained out of the storage at discharging and the energy fed in at charging process. The operation of this plant makes some additional components necessary, such as heat storage, after cooler, throttle, etc. which cause additional losses. In [11] the storage efficiency is calculated by the thermal efficiency of the combined cycle process with and without storage operation.

The thermal efficiency of the GT-26 is calculated with the results of a separate stationary simulation of this combined cycle process.

$$\eta_{cc} = \frac{P_{tur} - P_{com} - P_{pum}}{P_{ng}} \tag{58}$$

$$\eta_{cc} = \frac{810,36\ MW - 363,4\ MW - 1,96\ MW}{753,35\ MW} \tag{59}$$

$$\eta_{cc} = 0,5907 \tag{60}$$

The thermal efficiency with additional compressor and combustion chamber in storage mode:

$$\eta_{cc,sto} = \frac{E_{tur} - E_{com,ent} - E_{pum}}{E_{ng,ent}} \tag{61}$$

$$\eta_{cc,sto} = \frac{17,547\ TJ - 8,503\ TJ - 0,041\ TJ}{18,140\ TJ} \tag{62}$$

$$\eta_{cc,sto} = 0,4963 \tag{63}$$

The storage efficiency is defined as ratio of η_{cc} and $\eta_{cc,sto}$ considering the additional components needed as storage losses. The storage efficiency equates to:

$$\eta_{sto} = \frac{\eta_{cc,sto}}{\eta_{cc}} \tag{64}$$

$$\eta_{sto} = \frac{0,4963}{0,5907} \tag{65}$$

$$\eta_{sto} = 0,8402 \tag{66}$$

The plant efficiency is calculated with the ratio of the overall power in- and output:

$$\eta_{plant} = \frac{E_{tur}}{E_{com,ent} + E_{pum} + E_{ng,ent}} \tag{67}$$

$$\eta_{plant} = \frac{17,547\ TJ}{8,503\ TJ + 0,041\ TJ + 18,140\ TJ} \tag{68}$$

$$\eta_{plant} = 0,6576 \tag{69}$$

The storage capacity is calculated with the electrical output, runtime and the storage volume:

$$c = \frac{P_{out} \cdot t_{sto}}{V_c} = \frac{812 \cdot 10^3\ kW_{out} \cdot 6\ h}{264.327\ m^3}$$
$$c = 18,43\ \frac{kWh_{out}}{m^3} \tag{70}$$

Compared to the CAES-plants Huntorf and McIntosh the calculated values represent an considerable raise in efficiency and storage capacity.

4 Conclusion

In the presented paper the modelling and simulation of an underground cavern in a salt dome combined with a brine shuttle pond at the surface for nearly isobaric operation is described and examined. This model enables to simulate the dynamic operation of the ISACOAST-CC (isobaric adiabatic compressed air energy storage plant with combined cycle) concept developed at the Institute for Heat- and Fuel Technology with the cycle simulation software ENBIPRO.

The same energy balance (without volume change work) is used in another cavern model with constant volume, which is used to simulate the operation of the Huntorf CAES-plant. The results have been validated by comparison with operational data of this cavern. Further development of the presented model is required, regarding the heat losses inside the tubings or dynamic adaptation of the pressure loss coefficients which is not implemented so far.

The different component models such as compressor, turbine, combustion chamber and steam turbine used in the dynamic simulation of the ISACOAST-CC storage cycle were validated with the cycle simulation software Gatecycle. As a result, a significant raise in efficiency is achieved and the simulation demonstrates the theoretical feasibility with high flexibility of this CAES-plant. The innovative concept is an advancement of state-of-the-art CAES-plants and represents a further important step for a sustainable power supply based on renewable energies.

Acknowledgements: The project this report is based on is funded by E.ON AG as part of the E.ON Research Initiative. Responsibility for the content of this publication lies with the authors.

We would like to express our gratitude to the E.ON AG for the financial sponsorship and technical assistance in the ISACOAST-CC project, as well as KBB Underground Technologies GmbH.

Nomenclature

Symbol	Unit	Description
a	$\frac{m^2}{s}$	conductibility of temperature
A	m^2	area
A_e	$-$	surface enlargement factor
Bi^+	$-$	Biot-number
c	$\frac{kWh_{out}}{m^3}$	specific storage capacity
c_p	$\frac{J}{kgK}$	specific heat capacity at const. pressure
c_v	$\frac{J}{kgK}$	specific heat capacity at const. volume
d	m	diameter
E	TJ, GWh	energy
Fo^+	$-$	Fourier-number
g	$\frac{m}{s^2}$	gravity
h	$\frac{J}{kg}$	specific enthalpy
H	m	height
m	kg	mass
n	$-$	polytropic exponent
P	MW, kW	power
p	Pa	pressure
$\tilde{\dot{q}}_i$	$\frac{W}{m^3}$	inner heat source
$\dot{Q}$	W	heat flow
R	$\frac{J}{kgK}$	specific gas constant
r	m	radius
r^*	$-$	dimensionless location coordinate
t	s, h	time
T	K	temperature
u	$\frac{J}{kg}$	specific inner energy
v	$\frac{m}{s}$	velocity
V	m^3	volume
$\dot{W}_t$	W	flow of technical work
$\dot{W}_v$	W	flow of volume change work
z	m	height, filling level
α	$\frac{W}{m^2K}$	heat transfer coefficient
Δ	$-$	difference
ζ	$-$	pressure loss coefficient
η	$-$	efficiency
ρ	$\frac{kg}{m^3}$	density
τ	s	time

Index	Description
a	air
b	brine
cc	combined cycle
c	cavern
com	compressor
cv	control volume
d	depth
el	electric
ent	entire
env	environment
gt	gas turbine
i	timestep
j	location
in	inlet
m	mean
ng	natural gas
out	outlet
pol	polytropic
pum	pump
rs	rock salt
st	steam turbine
sto	storage
tur	turbine
$\emptyset$	cross section
∞	infinity

References:

[1] Deutsche Energie-Agentur GmbH (dena), *Energiewirtschaftliche Planung für die Netzintegration von Windenergie in Deutschland an Land und Offshore bis zum Jahr 2020*, Köln, 24.02.05

[2] F. Crotogino, *Druckluftspeicher-Kraftwerke zum Ausgleich fluktuierender Windenergie / Stand der Technik und neue Entwicklungen*, lecture on the 6th Windenergy-Forum Flensburg, 20.04.06

[3] B. Calaminus, *Innovatives Druckluftspei–cherkraftwerk der EnBW*, lecture on the occassion of the Energietage Hannover, 31.10.07

[4] C. Schlitzberger, R. Leithner and L. Nielsen *Isobares GuD - Druckluftspeicherkraftwerk mit Wärmespeicher*, Kraftwerkstechnisches Kolloquium Dresden, 2008

[5] B. Epple, R. Leithner, W. Linzer and H. Walter *Simulation von Kraftwerken und wärmetechnischen Anlagen*, Springer Verlag, 2009, ISBN: 978-3-211-29695-0

[6] H. Zindler, A. Hauschke, H. Walter and R. Leithner *Dynamic Simulation of a 800 MWel Hard*

Coal One-Through Supercritical Power Plant to Fulfill the Great Britain Grid Code, Proceedings of the 6th IASME/WSEAS International Conference on Heat Transfer, Thermal Engineering and Environment (HTE'08), Rhodes, Greece, 2008, ISBN: 978-3-211-29695-0

[7] A. Hauschke and R. Leithner *Dynamic Simulation of Fouling and Optimization of Sootblowing Intervals in a Hard Coal Fired Power Plant*, Proceedings of the 5th International Conference on Energy, Environment, Ecosystems and Sustainable Development (EEESD '09), Athens, Greece, 2009, ISBN: 978-960-474-125-0

[8] H. Zindler, A. Hauschke and R. Leithner *Impact of the HP Preheater Bypass on the Economizer Inlet Header*, Proceedings of the 5th International Conference on Energy, Environment, Ecosystems and Sustainable Development (EEESD '09), Athens, Greece, 2009, ISBN: 978-960-474-125-0

[9] J. Köhler, *Skriptum zur Vorlesung Thermodynamik I*, Institute for Thermodynamics, Techni–sche Universität Braunschweig, 2002

[10] N. Elsner, S. Fischer and J. Huhn, *Grundlagen der technischen Thermodynamik, Band 2 Wärmeübertragung*, Akademie Verlag, 1993

[11] L. Nielsen, *Analysis, technical and economical optimization of energy-storage plants through dynamical simulation*, Master thesis, Institute for Heat- and Fuel Technology, Technische Universität Braunschweig, 2008